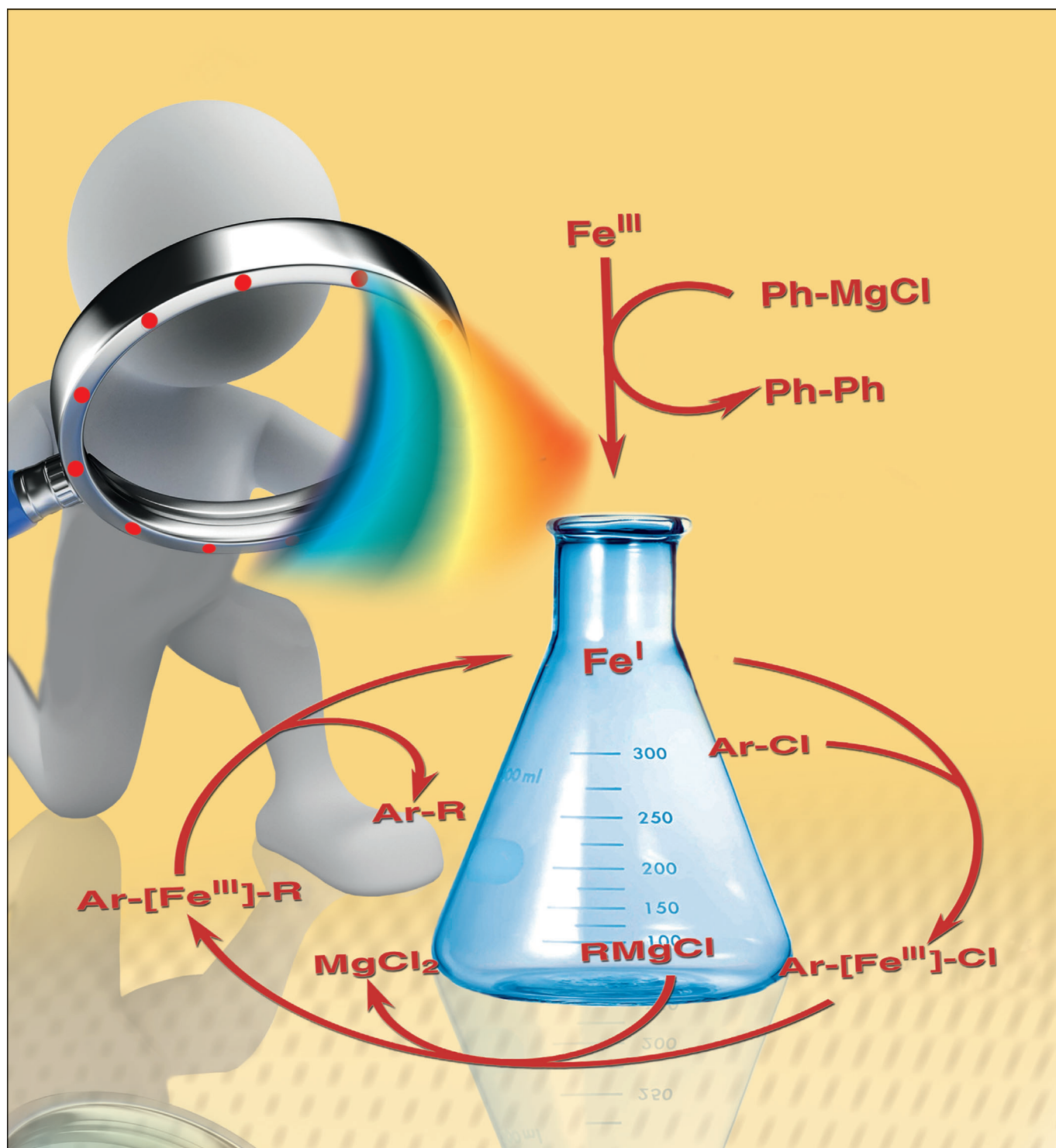


# X-ray Spectroscopic Verification of the Active Species in Iron-Catalyzed Cross-Coupling Reactions

Roland Schoch,<sup>[a]</sup> Willi Desens,<sup>[b]</sup> Thomas Werner,<sup>\*,[b]</sup> and Matthias Bauer<sup>\*,[a]</sup>



Over the past two decades iron catalysis has become a powerful tool in organic synthesis.<sup>[1]</sup> Cross-coupling reactions doubtless rank among the most important of these reactions, because they allow effective formation of carbon scaffolds.<sup>[1,4h-q,2]</sup> Nowadays, these transformations are a standard tool for the preparation of fine chemicals and biologically active compounds on both laboratory and industrial scales.<sup>[1d]</sup> Although cross-coupling reactions are dominated by palladium complexes, iron complex catalysts offer an alternative of increasing importance due to their easy accessibility, short reaction times and broad functional group tolerance.<sup>[1b,g]</sup> Under established conditions alkyl or aryl Grignard reagents are coupled with aryl chlorides, triflates and tosylates.<sup>[1e,g,n,2a,3a]</sup>

Despite the importance of iron-catalyzed cross-coupling reactions and intensive investigations, the mechanism of this reaction is still subject to ongoing discussion.<sup>[1m,3]</sup> Spectroscopic studies are very limited due to the paramagnetic character of the species formed.<sup>[3a]</sup> Hence, mechanistic findings are mainly based on investigations of potential intermediates.<sup>[3a]</sup> In contrast to palladium-catalyzed cross-couplings, for which detailed mechanistic knowledge exists,<sup>[4]</sup> this gap prevents the directed development of improved iron catalysts for cross-coupling reactions.

X-ray absorption spectroscopy represents a method to bridge this gap.<sup>[5]</sup> It provides element specific clarification of local structure and oxidation state of metal centers through EXAFS (extended X-ray absorption fine structure) and XANES (X-ray absorption near edge structure) spectroscopy.<sup>[6]</sup> Employing these methods, the type and number of ligands as well as their distance from the catalytically active metal center can be determined *in situ*.<sup>[7]</sup> Despite these advantages, which were already used for investigations of different cross-coupling and Grignard reactions,<sup>[5,8]</sup> to the best of our knowledge no XAS investigations on iron-catalyzed cross-coupling reactions have been reported to date. This is even more surprising, because this type of investigation would enable a comparison of the five suggested mechanisms proposed to date for this type of cross-coupling:<sup>[3a]</sup>

- 1) Kochi et al.<sup>[9]</sup> postulate a “soluble iron species” of unspecified oxidation state, which exists as an aggregate complexed by Grignard compounds. In this case, Fe–Fe pairs characteristic of a metal cluster would be expected in the EXAFS analysis.

[a] R. Schoch, Prof. Dr. M. Bauer  
Fachbereich Chemie, TU Kaiserslautern  
Erwin-Schrödinger-Str. 54, 67663 Kaiserslautern (Germany)  
Fax: (+49) 631-205-4676  
E-mail: bauer@chemie.uni-kl.de

[b] W. Desens, Dr. T. Werner  
Leibniz-Institut für Katalyse e.V. an der Universität Rostock  
Albert-Einstein-Str. 29a, 18059 Rostock (Germany)  
Fax: (+49) 381-1281-51326  
E-mail: thomas.werner@catalysis.de

Supporting information for this article is available on the WWW under <http://dx.doi.org/10.1002/chem.201303340>.

- 2) Bogdanovic et al.<sup>[10]</sup> suggest a heterobimetallic inorganic Grignard complex  $[\text{Fe}^{-\text{II}}(\text{MgCl})_2]_n$ , which would show Fe–Mg pairs in the EXAFS spectrum.
- 3) Fürstner et al.<sup>[11]</sup> describe the formation of Fe<sup>II</sup> organoferrates  $[\text{R}_n\text{Fe}^{+\text{II}}]^{2-n}$ . This type of compound would exhibit only Fe–C contributions to the radial distribution function.
- 4) Noda et al.<sup>[12]</sup> propose diaryl Fe<sup>II</sup> compounds stabilized by TMEDA, which would show similar EXAFS characteristics to the organoferrates described in point 3).
- 5) Norrby et al.<sup>[3b]</sup> suppose a catalytically active Fe<sup>I</sup>-species, which is not further structurally specified.

Herein, these proposals will be discussed on the basis of X-ray-spectroscopic investigations. According to the literature,<sup>[10]</sup> a maximum amount of four equivalents Grignard compound are required to form the active iron species. Analogously, the reaction products of iron(III)-acetylacetonate  $\text{Fe}(\text{acac})_3$  and one to four equivalents phenylmagnesiumchloride  $\text{PhMgCl}$  in THF/NMP were examined to identify the species formed through activation of the pre-catalyst  $\text{Fe}(\text{acac})_3$ .<sup>[13]</sup>

Figure 1 shows the energy-calibrated XANES spectra during addition of 1–4 equivalents of  $\text{PhMgCl}$  to  $\text{Fe}(\text{acac})_3$  in THF/NMP. To emphasize small changes, the first derivatives<sup>[14]</sup> of the spectra are displayed as well. Two spectral regions can be distinguished: The pre-edge signal (prepeak)<sup>[15]</sup> at an energy of 7.10–7.11 keV (signal A) and the absorptions edge at a range of 7.11–7.12 keV (signals B and C). The prepeak position of the pre-catalyst  $\text{Fe}(\text{acac})_3$  is located at 7.106 keV and shifts after addition of one equivalent  $\text{PhMgCl}$  to a smaller value of 7.104 keV. Whereas this prepeak is caused by a  $1s \rightarrow 3d$  transition, the decreased resonance energy reflects the transition from an  $s^0d^5$  to an  $s^0d^6$  electron configuration, which corresponds to a reduction from Fe<sup>III</sup> to Fe<sup>II</sup>. This energy does not change with addition of further equivalents, but the prepeak intensity and the shape and energy of the absorption edge (signals B and C)

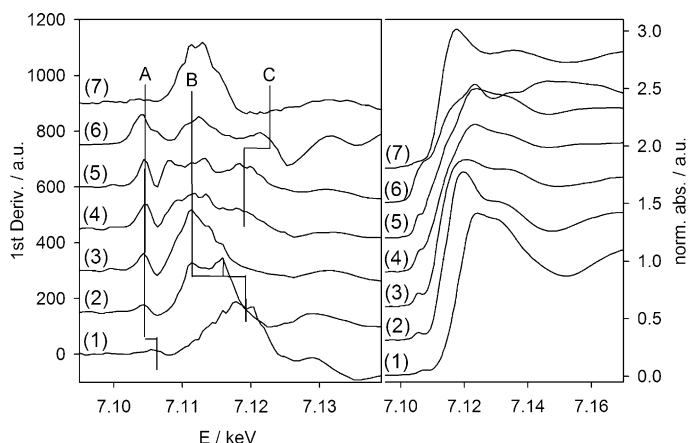


Figure 1. XANES spectra (right) and their derivatives (left) of the pre-catalyst  $\text{Fe}(\text{acac})_3$  (1) and after addition of one to four equivalents (2–5)  $\text{PhMgCl}$  in comparison to  $\text{Fe}^0$  (6) and under reaction conditions (7).

changes in a systematic way. The first derivative of the pre-catalyst spectra shows only one signal (B), which shifts significantly in energy after addition of one equivalent of PhMgCl and then exhibits an Fe<sup>II</sup> characteristic doublet structure.<sup>[14]</sup> With addition of the second equivalent, the higher-energetic signal of the doublet disappears. A related spectrum to the resulting first derivative is not known in the literature so far. With addition of three equivalents, another signal appears in the derivative, which can also be found in the spectrum of an iron foil (Fe<sup>0</sup>). The addition of the fourth equivalent causes no further changes in the spectrum, indicating that the activation of the catalyst is finished after the addition of three equivalents PhMgCl.

Although the XANES spectra of the active species might lead to speculation about a metalloide species due to the presence of the signals A, B and C, the shape and position of the signals deviate from that of an Fe<sup>0</sup> species. Even size-effects do not cause considerable changes in spectra of Fe<sup>0</sup> nanoparticles compared with spectra of a bulk Fe foil.<sup>[16]</sup> Hence the broadened shape of the prepeak signal is not the result of Fe<sup>0</sup> nanoparticle formation.<sup>[17]</sup> The rather distinct separation of the prepeak from the main-edge indicates a certain ionic character. Because the Fe<sup>0</sup> and Fe<sup>II</sup> oxidation states can be excluded due to the XANES shape, the spectra of three and four equivalents of PhMgCl are thus assigned to an oxidation state of Fe<sup>I</sup>, in keeping with the findings of Adams et al. in iron-catalyzed Negishi reactions.<sup>[18]</sup>

This argument is supported by quantification of the organic redox product biphenyl (Ph–Ph). It is formed by an oxidative coupling of two Ph<sup>–</sup> during the reduction of Fe<sup>III</sup>. Because β-hydride elimination can be excluded as side path, the number of electrons transferred to iron can be determined by quantification of the Ph–Ph formed by means of gas chromatography.<sup>[19]</sup> Because no organo-halide is present

as potential coupling reagent at this stage, reversible redox-pairs can be excluded.<sup>[18]</sup> Fe(acac)<sub>3</sub> was treated with 1–10 equiv PhMgCl and the resulting reaction mixtures were analyzed by quantitative GC.<sup>[20]</sup> In presence of one equivalent of PhMgCl, full conversion to biphenyl was observed. It is likely, that the phenyl-anion reduced Fe<sup>III</sup> to Fe<sup>II</sup> under formation of a phenyl-radical, two of which can couple forming the biphenyl observed. Analogous homo-couplings of Grignard compounds in presence of Fe<sup>III</sup>-complexes have already observed.<sup>[18,20]</sup> With the addition of two equivalents of PhMgCl, only 65 % of the theoretical amount of biphenyl is formed through reduction of Fe<sup>III</sup> to Fe<sup>I</sup> (Table 1, entry 2). This suggests a formal alteration of the oxidation state from +3 to +1.7. In contrast, the addition of three equivalents of Grignard reagent leads to a formal change in oxidation state from +3 to +1. If one equivalent of Fe(acac)<sub>3</sub> is converted with an excess of four or ten equivalents PhMgCl, only small differences in the formed oxidation states are visible compared to addition of three equivalents.

The trends observed in the XANES spectra and the results of the GC investigations are reflected in the EXAFS spectra as shown in Figure 2. The nuclearity of the iron compound formed during the activation process and the nature of the ligands coordinated to the metal core can both be extracted from the EXAFS spectra. In course of the activation, the EXAFS signal is dominated by iron–iron contributions because of the high backscattering amplitude of iron. The coordination number of iron follows no regular behavior, as can be seen in Table 1. Based on the Fe–Fe coordination number of 0.7 obtained after reaction with one equivalent of PhMgCl the formation of dimers can be deduced. The iron–iron distance of 2.55 Å is consistent with the partial reduction of the iron centers deduced from the XANES spectra and literature values (2.46–2.69 Å) for Fe<sup>II</sup> dimers

Table 1. Structural parameters, obtained through fitting of the experimental EXAFS spectra.

Entry	Sample	Abs–Bs <sup>[a]</sup>	N(Bs) <sup>[b]</sup>	R(Bs) <sup>[c]</sup> [Å]	σ <sup>[d]</sup> [Å]	R <sup>[e]</sup> [%]	Transferred e <sup>–</sup> oxidation state of Fe
1	Fe(acac) <sub>3</sub>	Fe–O(acac)	6	1.99 ± 0.02	0.067 ± 0.007	24.10	–
		Fe–C	6	2.93 ± 0.03	0.084 ± 0.008		
2	+1 equiv PhMgCl	Fe–O(acac)	3.9 ± 0.2	2.04 ± 0.02	0.081 ± 0.004	19.85	1.0 equiv
		Fe–O(THF/NMP)	2.0 ± 0.2	2.20 ± 0.02	0.039 ± 0.004		+2.0
		Fe–Fe	0.7 ± 0.3	2.55 ± 0.03	0.100 ± 0.040		
3	+2 equiv PhMgCl	Fe–C(Ph)	1.4 ± 0.1	1.94 ± 0.02	0.112 ± 0.011	7.97	1.3 equiv
		Fe–O(THF/NMP)	0.4 ± 0.1	2.19 ± 0.02	0.032 ± 0.003		+1.7
		Fe–Fe	5.1 ± 0.5	2.42 ± 0.02	0.102 ± 0.010		
		Fe–Mg	1.6 ± 0.3	2.74 ± 0.03	0.097 ± 0.040		
4	+3 equiv PhMgCl	Fe–C(Ph)	1.1 ± 0.1	1.97 ± 0.02	0.032 ± 0.003	23.32	2.0 equiv
		Fe–O(THF/NMP)	1.5 ± 0.1	2.07 ± 0.02	0.039 ± 0.004		+1.0
		Fe–Fe	2.0 ± 0.4	2.55 ± 0.03	0.112 ± 0.011		
		Fe–Mg	0.5 ± 0.3	2.62 ± 0.03	0.032 ± 0.015		
5	+4 equiv PhMgCl	Fe–C(Ph)	0.8 ± 0.1	1.95 ± 0.02	0.059 ± 0.006	19.03	2.3 equiv
		Fe–O(THF/NMP)	1.4 ± 0.1	2.10 ± 0.02	0.032 ± 0.003		+0.7
		Fe–Fe	2.6 ± 0.4	2.52 ± 0.02	0.112 ± 0.011		
		Fe–Mg	1.0 ± 0.3	2.59 ± 0.03	0.050 ± 0.015		
7	Reaction cond. (+4 equiv PhMgCl + 10 equiv <b>1b</b> )	Fe–C(Ph)	1.5 ± 0.1	1.93 ± 0.02	0.112 ± 0.011	10.29	–
		Fe–O(THF/NMP)	0.4 ± 0.1	2.14 ± 0.02	0.045 ± 0.004		
		Fe–Fe	6.7 ± 0.4	2.44 ± 0.02	0.100 ± 0.040		
		Fe–Mg	1.8 ± 0.3	2.80 ± 0.03	0.097 ± 0.040		

[a] Abs = X-ray absorbing atom, Bs = backscatterer (neighbor atom). [b] Number of neighbor atoms; italicized numbers are crystallographic values. [c] Distances Abs–Bs. [d] Debye–Waller factor, considers static and vibronic disorder. [e] Quality of the fit.

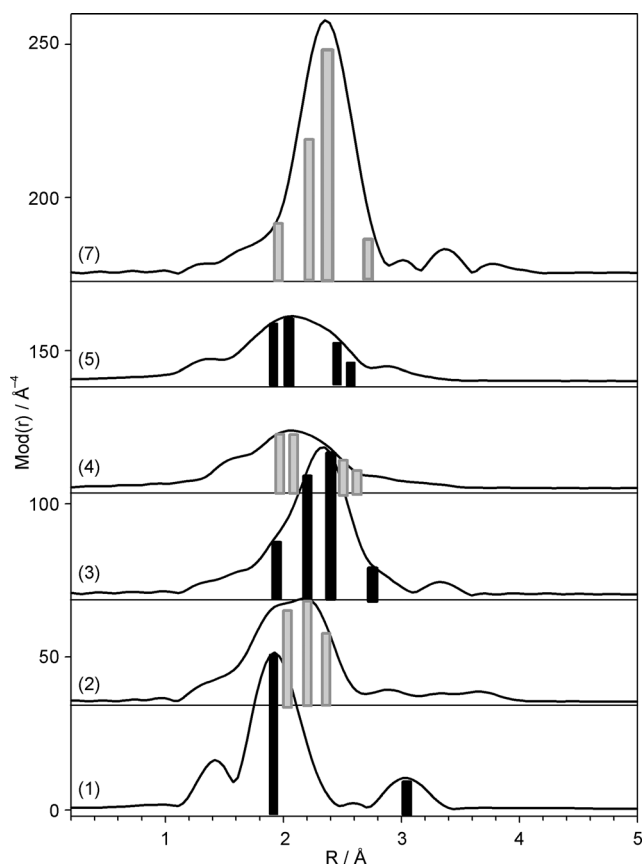


Figure 2. Fourier-transformed EXAFS spectra of the pre-catalyst  $\text{Fe}(\text{acac})_3$  (1) after addition of one to four equivalents  $\text{PhMgCl}$  (2–5) and under reaction conditions (7) with 2-chloropyridine as coupling reagent. The constitutive shells are indicated as bars.<sup>[21]</sup>

with direct Fe–Fe contact and bridging C- or N-containing ligands (e.g.,  $[\text{Fe}(\text{mes})_2]_2$  or  $[\text{Fe}(\text{tim})_2]_2$ ).<sup>[22]</sup> With two equivalents  $\text{PhMgCl}$  the number of iron–iron contacts increases to 5.1. Thereby the presence of iron-clusters with a size of  $13 \pm 2$  atoms can reasonably be assumed.<sup>[23]</sup> GC quantification of the biphenyl formed, suggests a formal oxidation number of  $+1.7$ .<sup>[23]</sup> A fractional oxidation number, such as 1.7, cannot be realized in a molecular compound and supports the cluster formation hypothesis. The iron–iron distance of  $2.42 \text{ \AA}$  extracted, on the other hand, is in the lower range of documented values for multinuclear  $\text{Fe}^{\text{II}}$  compounds<sup>[24]</sup> and supports the ascertained number electrons transferred. Surprisingly, the addition of three and four equivalents  $\text{PhMgCl}$  causes a decrease in aggregation from  $\text{Fe}_{13}$  to  $\text{Fe}_{3-4}$ . The oxidation state determined from GC analysis is  $\text{Fe}^{\text{I}}$ , which is verified by the Fe–Fe distance of  $2.53 \text{ \AA}$ .<sup>[25]</sup> In general the error in the determination of the iron core size by EXAFS spectroscopy is small, because the Fe–Fe coordination number excludes the presence of larger clusters.

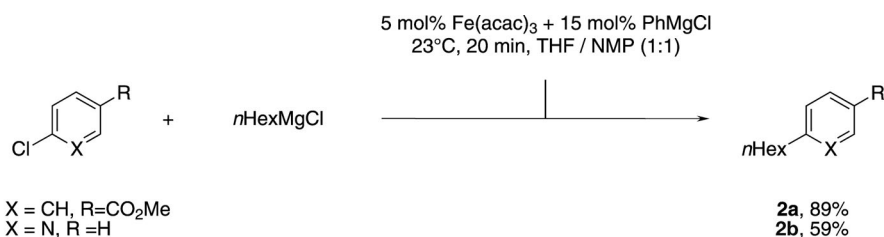
Besides Fe–Fe pairs, contributions of the lighter atoms present (Table 1) also provide information about the ligands stabilizing the iron core. After addition of one equivalent of  $\text{PhMgCl}$ , Fe–O contributions are found, which can be assigned to the pre-catalyst  $\text{Fe}(\text{acac})_3$ .<sup>[26]</sup> Because all  $\text{PhMgCl}$

was consumed by the formation of Ph–Ph, the coordination of phenyl residues can be excluded. The coordination number of four determined agrees well with UV/Vis measurements, which indicated that 65% Fe–O(acac) signal remained.<sup>[27]</sup> In addition to the first Fe–O shell, a second contribution of a lighter backscatterer at a distance of  $2.2 \text{ \AA}$  could be detected, which is attributed to bridging, neutral ligands like THF or NMP.<sup>[28]</sup> NMP is known to stabilize small nanoparticles.<sup>[29]</sup> Further contributions, which could indicate coordinating MgX groups, were not found after addition of one equivalent of  $\text{PhMgCl}$ . This changes with addition of the second equivalent  $\text{PhMgCl}$ . Raman and UV/Vis-measurements detect only marginal Fe–O(acac) contributions.<sup>[30]</sup> An Fe–C bond with a length of  $1.94 \text{ \AA}$  can be deduced, which suggest an average of 1.4 coordinating phenyl residues.<sup>[31]</sup> The sterically demanding aryl groups coordinate to  $\text{Fe}^{\text{I}}$  at a distance of  $2.0 \text{ \AA}$ .<sup>[18,32]</sup> Because 1.3 equivalents of phenyl anion were consumed forming Ph–Ph, 0.7 equivalents remain formally available. To obtain an EXAFS coordination number of 1.4, the phenyl groups must act as bridging ligands. Furthermore, every iron center is stabilized by 1.6 Mg atoms at a distance of  $2.74 \text{ \AA}$ , which can be attributed to Fe–Mg(–Cl) according to literature.<sup>[10]</sup> The coordination is complemented through coordination of 0.5 THF/NMP ligands at a distance of  $2.2 \text{ \AA}$ .<sup>[28b]</sup>

Although addition of a third equivalent  $\text{PhMgCl}$  causes significant alterations in the Fe–Fe core, the coordination numbers in the ligand shells change only slightly. The number of coordinating  $\text{Ph}^-$  residues decrease to one because two equivalents of  $\text{Ph}^-$  are consumed in reduction process the Fe–C coordination number obtained by EXAFS coincides exactly with the quantitative GC analysis results. In contrast, the number of THF/NMP ligands increases slightly, whereas their distance from the Fe–Fe core decreases by  $0.12$  to  $2.07 \text{ \AA}$ . These Fe–O distances are known for ether compounds coordinating on low-valent iron-centers.<sup>[8a,b]</sup> The Fe–Mg coordination number decreases to 0.5 when three equivalents of  $\text{PhMgCl}$  are used, accompanied by a shorter bond length of  $2.62 \text{ \AA}$ . This relatively short distance is characteristic for a strong covalent interaction between magnesium ligands and an  $\text{Fe}_3$  core.<sup>[8a,33]</sup>

Through addition of a fourth equivalent of  $\text{PhMgCl}$ , no further structural changes were observed. The results of the EXAFS analysis correspond to the XANES evaluation. Both methods together with GC analysis, Raman and UV/Vis spectroscopy demonstrate that only three equivalents of reduction reagent  $\text{PhMgCl}$  are necessary to form the catalytically active species. Furthermore the data show that in contrast to iron-catalyzed Negishi couplings, the active species is not characterized by Fe–X ( $\text{X} = \text{Cl}^-$ ,  $\text{Br}^-$ ) bonds, but by Fe–R ( $\text{R} = \text{Ph}^-$ ) bonds.<sup>[18]</sup>

Finally, after structural determination of the species formed in the activation process, the catalytic activity of these species was demonstrated. Hereto 5 mol%  $\text{Fe}(\text{acac})_3$  were converted with 15 mol%  $\text{PhMgCl}$  (Scheme 1). In presence of the in situ formed catalyst a cross-coupling reaction between aryl halide **1a** and  $n\text{HexMgCl}$  to form product **2a**

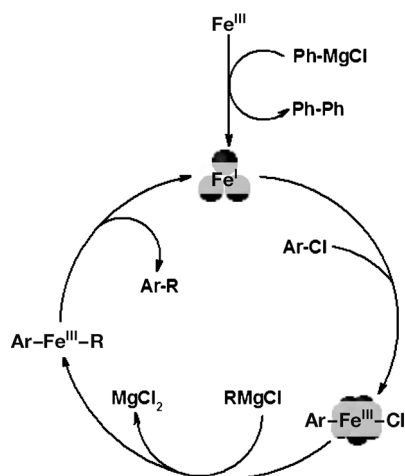


Scheme 1. Test reactions and yields.

with a yield of 89% could be conducted. The yield of an analogous reaction with *n*HexMgBr is documented with 91% yield in ref. [2a]. In general, cross-coupling of heterocyclic compounds with *n*HexMgCl is possible under similar reaction conditions. The conversion of the pyridine derivative **1b** leads to product **2b** in moderate yield of 59% (Scheme 1). However, with *n*HexMgBr a 91% yield could be achieved.<sup>[34]</sup>

The XANES spectrum of the spectroscopic “resting state” under reaction conditions as applied in the first example is shown in Figure 1. It displays the same spectral signatures as the spectrum of an Fe<sup>II</sup> species with two equivalents PhMgCl. Nevertheless, EXAFS data imply the formation of larger nanoparticles as indicated by a higher Fe–Fe coordination number.

Although XAS only gathers the average spectra of all species present in the reaction mixture, the mechanism displayed in Scheme 2 can be deduced based on the spectroscopic and catalytic data presented. In the first step the pre-catalyst Fe(acac)<sub>3</sub> is reduced to the catalytically active Fe<sup>I</sup> species with an oxidation state. Subsequently an oxidative addition of the organohalide occurs, associated with a change of the oxidation state from Fe<sup>I</sup> to Fe<sup>III</sup>. The spectroscopic observation of Fe<sup>II</sup> substantiates the presence of Fe nanoparticles in this case. In their core, Fe<sup>I</sup> centers persist. Averaged with the Fe<sup>III</sup> centers from the oxidative addition on the particle surface this yields a mean oxidation



Scheme 2. Proposed mechanism of Fe-catalyzed cross-coupling reactions.

state of Fe<sup>II</sup>. The averaged Fe–Fe coordination number corresponds to a cluster diameter of approximately 10 Å.<sup>[23c]</sup> Clusters of that size exhibit a surface atom (Fe<sup>III</sup>) to bulk atom (Fe<sup>I</sup>) ratio of 1:1,<sup>[35]</sup> which would result in an observed Fe<sup>II</sup>.

Subsequent transmetalation and ensuing reductive elimination with release of the product and regeneration of the active catalyst has not been experimentally demonstrated so far, but is certainly plausible. Based on XAS results, a composition of Fe<sub>3</sub>(MgCl)<sub>3</sub>L<sub>3</sub> is possible. The oxidation state obtained from XANES spectra and GC analysis is Fe<sup>I</sup>, which is in agreement with the recent study of Norrby et al. who also found that the Grignard reagent alone can only reduce the iron pre-catalyst to Fe<sup>I</sup>.<sup>[36]</sup>

The XAS results presented allow the assessment of the non-spectroscopic mechanistic studies of iron cross-coupling reactions reported to date. Based on the oxidation state of Fe<sup>I</sup> for the active species determined by XANES and GC analysis, it is possible to preclude hypotheses 2,<sup>[10]</sup> 3<sup>[11]</sup> and 4,<sup>[12]</sup> because these species have oxidation states of –II and +II. Nevertheless the suggestion of Bogdanovic et al.<sup>[10]</sup> postulates a structure element with an Fe–Mg bond, which was also advanced by Kochi.<sup>[9]</sup> The proposal assumes an agglomeration, the extent of which could only be demonstrated to be very small by the EXAFS results described herein. The oxidation state found agrees with that established by Norrby.<sup>[36]</sup>

Comparisons with related studies<sup>[37]</sup> suggest that the oxidation state of the active species depends on the nature of the Grignard reagent, which is based on coordination of the organic Grignard reagent. Further systematic studies to this point are planned for the near future.

## Experimental Section

X-ray absorption measurements were carried out at beamlines XAS and X1 at the synchrotrons ANKA (Karlsruhe) and HASYLAB (Hamburg). All measurements at the Fe K edge (7.112 keV) were performed in transmission under application of a Si(111) double crystal monochromator and N<sub>2</sub>-filled ionization chambers in a cell, which allows for work under inert conditions. Details of the experimental procedure and treatment of the data are found in the Supporting Information, as well as details of the GC analysis and sample preparation.

## Acknowledgements

M.B. gratefully acknowledges financial support of the Carl-Zeiss foundation and the Landesforschungsschwerpunkt Rheinland-Pfalz Nanokat. Additionally, beamtime provision by HASYLAB (Hamburg) and ANKA (Karlsruhe) is acknowledged as well as support by Dr. E. Welter and Dr. S. Mangold.

**Keywords:** cross-coupling • EXAFS • homogeneous catalysis • iron • reaction mechanisms • XANES

- [1] a) C. Bolm, J. Legros, J. Le Paih, L. Zani, *Chem. Rev.* **2004**, *104*, 6217–6254; b) W. M. Czaplik, M. Mayer, J. Cvengros, A. J. von Wangelin, *ChemSusChem* **2009**, *2*, 396–417; c) *Iron Catalysis in Organic Chemistry* (Ed.: B. Plietker), Wiley-VCH, Weinheim, **2008**; d) M. Beller, A. Zapf, W. Mägerlein, *Chem. Eng. Technol.* **2001**, *24*, 575–582; e) O. M. Kuzmina, A. K. Steib, D. Flubacher, P. Knochel, *Org. Lett.* **2012**, *14*, 4818–4821; f) R. Martin, A. Fürstner, *Angew. Chem.* **2004**, *116*, 4045–4047; *Angew. Chem. Int. Ed.* **2004**, *43*, 3955–3957; g) E. Nakamura, N. Yoshikai, *J. Org. Chem.* **2010**, *75*, 6061–6067; h) R. B. Bedford, E. Carter, P. M. Cogswell, N. J. Gower, M. F. Haddow, J. N. Harvey, D. M. Murphy, E. C. Neeve, J. Nunn, *Angew. Chem.* **2013**, *125*, 1323–1326; *Angew. Chem. Int. Ed.* **2013**, *52*, 1285–1288; i) D. Castagnolo, M. Botta, *Eur. J. Org. Chem.* **2010**, 3224–3228; j) S. K. Ghorai, M. Jin, T. Hatakeyama, M. Nakamura, *Org. Lett.* **2012**, *14*, 1066–1069; k) B. Scheiper, M. Bonnekeßel, H. Krause, A. Fürstner, *J. Org. Chem.* **2004**, *69*, 3943–3949; l) G. Seidel, D. Laurich, A. Fürstner, *J. Org. Chem.* **2004**, *69*, 3950–3952; m) A. Fürstner, A. Leitner, *Angew. Chem.* **2002**, *114*, 632–635; *Angew. Chem. Int. Ed.* **2002**, *41*, 609–612; n) A. Fürstner, M. Méndez, *Angew. Chem.* **2003**, *115*, 5513–5515; *Angew. Chem. Int. Ed.* **2003**, *42*, 5355–5515; o) S. Kawamura, T. Kawabata, K. Ishizuka, M. Nakamura, *Chem. Commun.* **2012**, *48*, 9376–9378; p) Z. Mo, Q. Zhang, L. Deng, *Organometallics* **2012**, *31*, 6518–6521.
- [2] a) A. Fürstner, A. Leitner, M. Méndez, H. Krause, *J. Am. Chem. Soc.* **2002**, *124*, 13856–13863; b) H. Shinokubo, K. Oshima, *Eur. J. Org. Chem.* **2004**, 2081–2091.
- [3] a) B. D. Sherry, A. Fürstner, *Acc. Chem. Res.* **2008**, *41*, 1500; b) J. Kleimark, A. Hedström, P.-F. Larsson, C. Johansson, P.-O. Norrby, *ChemCatChem* **2009**, *1*, 152–161; c) K. Weber, E.-M. Schnöckelborg, R. Wolf, *ChemCatChem* **2011**, *3*, 1572–1577; d) Q. Ren, S. Guan, F. Jiang, J. Fang, *J. Phys. Chem. A* **2013**, *117*, 756–764; e) J. K. Kochi, *J. Organomet. Chem.* **2002**, *653*, 11–19.
- [4] N. Miyauro, *Cross-Coupling Reactions: A Practical Guide; Topics in Current Chemistry*, Springer, Berlin, **2002**.
- [5] L. E. Aleandri, B. Bogdanović, C. Dürr, S. C. Hockett, D. J. Jones, U. Kolb, M. Lagarden, J. Rozière, U. Wilczok, *Chem. Eur. J.* **1997**, *3*, 1710–1718.
- [6] a) H. Bertagnolli, T. S. Ertel, *Angew. Chem.* **1994**, *106*, 15–37; *Angew. Chem. Int. Ed. Engl.* **1994**, *33*, 45–66; b) M. P. Feth, C. Bolm, J. P. Hildebrand, M. Köhler, O. Beckmann, M. Bauer, R. Ramamonjisoa, H. Bertagnolli, *Chem. Eur. J.* **2003**, *9*, 1348–1359.
- [7] a) M. Bauer, G. Heusel, S. Mangold, H. Bertagnolli, *J. Synchrotron Radiat.* **2010**, *17*, 273–279; b) M. Bauer, C. Gastl, *Phys. Chem. Chem. Phys.* **2010**, *12*, 5575–5584.
- [8] a) L. E. Aleandri, B. Bogdanovic, A. Gaidies, D. J. Jones, S. Liao, A. Michalowicz, J. Roziere, A. Schott, *J. Organomet. Chem.* **1993**, *459*, 87–93; b) W. Hörner, H. Bertagnolli, *J. Organomet. Chem.* **2002**, *649*, 128–135.
- [9] M. Tamura, A. Kochi, *J. Am. Chem. Soc.* **1971**, *93*, 1487–1489.
- [10] a) L. E. Aleandri, B. Bogdanovic, P. Bons, C. Dürr, A. Gaidies, T. Hartwig, S. C. Hockett, M. Lagarden, U. Wilczok, R. A. Brand, *Chem. Mater.* **1995**, *7*, 1153–1170; b) B. Bogdanovic, M. Schwickardi, *Angew. Chem.* **2000**, *112*, 4788–4790; *Angew. Chem. Int. Ed.* **2000**, *39*, 4610–4612.
- [11] A. Fürstner, R. Martin, *Chem. Lett.* **2005**, *34*, 624–629.
- [12] D. Noda, Y. Sunada, T. Hatakeyama, M. Nakamura, H. Nagashima, *J. Am. Chem. Soc.* **2009**, *131*, 6078–6079.
- [13] In scenario 2 a  $\beta$ -hydride elimination is assumed to be necessary to form the appropriate compound. However with R=Ph other mechanisms are also conceivable that may lead to this species. Therefore, scenario 2 should be regarded as a possible reaction mechanism in the present studies with R=Ph.
- [14] I. Arçon, J. Kolar, A. Kodre, D. Hanžel, M. Strlič, *X-Ray Spectrom.* **2007**, *36*, 199–205.
- [15] M. Wilke, F. Farges, P.-E. Petit, G. E. Brown, F. Martin, *Am. Mineral.* **2001**, *86*, 714–730.
- [16] F. Jiménez-Villacorta, E. Céspedes, M. Vila, A. Muñoz-Martín, G. R. Castro, C. Prieto, *J. Phys. D* **2008**, *41*, 2050091–2050098.
- [17] D. Bazin, J. J. Rehr, *J. Phys. Chem. B* **2003**, *107*, 12398–12402.
- [18] C. J. Adams, R. B. Bedford, E. Carter, N. J. Gower, M. F. Haddow, J. N. Harvey, M. Huwe, M. Á. Cartes, S. M. Mansell, C. Mendoza, D. M. Murphy, E. C. Neeve, J. Nunn, *J. Am. Chem. Soc.* **2012**, *134*, 10333–10336.
- [19] See Supporting Information for details.
- [20] M. P. Shaver, L. E. N. Allan, H. S. Rzepa, V. C. Gibson, *Angew. Chem.* **2006**, *118*, 1263–1266; *Angew. Chem. Int. Ed.* **2006**, *45*, 1241–1244.
- [21] Details of the data analysis can be found in the Supporting Information.
- [22] a) H. Müller, W. Seidel, H. Görls, *J. Organomet. Chem.* **1993**, *445*, 133–136; b) F. A. Cotton, L. M. Daniels, J. H. Matonic, C. A. Murillo, *Inorg. Chim. Acta* **1997**, *256*, 277–282; c) C. R. Hess, T. Weyhermüller, E. Bill, K. Wiegardt, *Angew. Chem.* **2009**, *121*, 3758–3761; *Angew. Chem. Int. Ed.* **2009**, *48*, 3703–3706; d) M. M. Olmstead, P. P. Power, S. C. Shoner, *Inorg. Chem.* **1991**, *30*, 2547–2551.
- [23] a) X. Liu, M. Bauer, H. Bertagnolli, E. Roduner, J. van Slageren, F. Philipp, *Phys. Rev. Lett.* **2006**, *97*, 2534011–2534014; b) A. I. Frenkel, C. W. Hills, R. G. Nuzzo, *J. Phys. Chem. B* **2001**, *105*, 12689–12703; c) A. Jentys, *Phys. Chem. Chem. Phys.* **1999**, *1*, 4059–4063; d) A. M. Beale, B. M. Weckhuysen, *Phys. Chem. Chem. Phys.* **2010**, *12*, 5562–5574.
- [24] A. Klose, E. Solari, C. Floriani, A. Chiesi-Villa, C. Rizzoli, N. Re, *J. Am. Chem. Soc.* **1994**, *116*, 9123–9135.
- [25] T. Nguyen, W. A. Merrill, C. Ni, H. Lei, J. C. Fettinger, B. D. Ellis, G. J. Long, M. Brynda, P. P. Power, *Angew. Chem.* **2008**, *120*, 9255–9257; *Angew. Chem. Int. Ed.* **2008**, *47*, 9115–9117.
- [26] J. Iball, C. H. Morgan, *Acta Crystallogr.* **1967**, *23*, 239–244.
- [27] See Figure SI3 in the Supporting Information.
- [28] a) M. Bauer, S. Müller, G. Kickelbick, H. Bertagnolli, *New J. Chem.* **2007**, *31*, 1950–1959; b) H. Felkin, P. J. Knowles, B. Meunier, *Chem. Commun.* **1974**, 44.
- [29] This is the result of additional XAS measurements, in which much larger particles are found when no NMP is used.
- [30] See Figures SI2 and SI3 in the Supporting Information.
- [31] a) A. Fürstner, R. Martin, H. Krause, G. Seidel, R. Goddard, C. W. Lehmann, *J. Am. Chem. Soc.* **2008**, *130*, 8773–8787; b) K. Jonas, L. Schieferstein, C. Krüger, Y.-H. Tsay, *Angew. Chem.* **1979**, *91*, 590–591; *Angew. Chem. Int. Ed. Engl.* **1979**, *18*, 550–551; c) G. S. D. King, *Acta Crystallogr.* **1962**, *15*, 243–251.
- [32] C. Ni, B. D. Ellis, J. C. Fettinger, G. J. Long, P. P. Power, *Chem. Commun.* **2008**, *0*, 1014–1016.
- [33] H. Felkin, P. J. Knowles, B. Meunier, *J. Organomet. Chem.* **1978**, *146*, 151–167.
- [34] A. Fürstner, A. Leitner, M. Méndez in Iron catalyzed cross coupling reactions of aromatic compounds, Vol. US 20030220498 A1, **2003**.
- [35] C. Batchelor-McAuley, C. E. Banks, A. O. Simm, T. G. J. Jones, R. G. Compton, *ChemPhysChem* **2006**, *7*, 1081–1085.
- [36] A. Hedström, E. Lindstedt, P.-O. Norrby, *J. Organomet. Chem.* DOI: 10.1016/j.jorganchem.2013.04.024.
- [37] A. Welther, M. Bauer, M. Mayer, A. Jacobi von Wangelin, *ChemCatChem* **2012**, *4*, 1088–1093.

Received: August 26, 2013  
Published online: October 21, 2013